

# Global Fire Season Severity Analysis and Forecasting

Leonardo N. Ferreira<sup>a</sup>, Didier A. Vega-Oliveros<sup>b</sup>, Liang Zhao<sup>b</sup>, Manoel F. Cardoso<sup>c</sup>, Elbert E. N. Macau<sup>a,d</sup>

<sup>a</sup>*Associated Laboratory for Computing and Applied Mathematics, National Institute for Space Research, São José Dos Campos - SP, Brazil.*

<sup>b</sup>*Department of Computing and Mathematics, University of São Paulo, Ribeirão Preto - SP, Brazil.*

<sup>c</sup>*Center for Earth System Science, National Institute for Space Research, Cachoeira Paulista - SP, Brazil.*

<sup>d</sup>*Institute of Science and Technology, Federal University of São Paulo, São José Dos Campos - SP, Brazil.*

---

## Abstract

Global fire activity has a huge impact on human lives. In recent years, many fire models have been developed to forecast fire activity. They present good results for some regions but require complex parametrizations and input variables that are not easily obtained or estimated. In this paper, we evaluate the possibility of using historical data from 2003 to 2017 of active fire detections (NASA's MODIS MCD14ML C6) and time series forecasting methods to estimate global fire season severity (FSS), here defined as the accumulated fire detections in a season. We used a hexagonal grid to divide the globe, and we extracted time series of daily fire counts from each cell. We propose a straightforward method to estimate the fire season lengths. Our results show that in 99% of the cells, the fire seasons have lengths shorter than seven months. Given this result, we extracted the fire seasons defined as time windows of seven months centered in the months with the highest fire occurrence. We define fire season severity (FSS) as the accumulated fire detections in a season. A trend analysis suggests a global decrease in length and severity. Since FSS time series are concise, we used the monthly-accumulated fire counts (MA-FC) to train and test the seven forecasting models. Results show low forecasting errors in some areas. Therefore we conclude that many regions present predictable variations in the FSS.

**Keywords:** Global fire activity, Wildfire, Fire season length, Fire severity, Climate change, Time series prediction

---

## 1. Introduction

Wildfires have a fundamental role in the environment and a huge impact on human lives. They affect the biodiversity, destroy forests and houses, change global climate, and put risks to human health. The significant fire-related variables are the climate, vegetation,

---

*Email addresses:* leonardo.ferreira@inpe.br (Leonardo N. Ferreira), davo@icmc.usp.br (Didier A. Vega-Oliveros), zhao@usp.br (Liang Zhao), manoel.cardoso@inpe.br (Manoel F. Cardoso), elbert.macau@inpe.br (Elbert E. N. Macau)

and human activity [1]. Forecasting fire activity brings many benefits. Predictions and projections are useful in the management and control of fire. In the last decades, some complex models have been developed to forecast fire activity [2]. These models require data from different sources like climate, population, land use, and lightning. For some regions, data are not available, which restricts their application. These models present satisfactory results for many regions but require difficult parametrization. Furthermore, some models cannot reproduce the pattern and magnitude of observed in the fire activity [3]. The central question behind this paper is to verify how effective are the time series forecasting methods on estimating the fire season severity using historical data.

In this paper, we analyze and predict global fire seasons severities, defined as is the sum of the fire counts detected in a season [4]. We use global fire count detections from 2003 to 2017 provided by the NASA. We applied a hexagonal grid to divide the globe and extract time series of active fire counts (FC) from each cell. First, we propose a simple method to estimate the fire seasons from these time series. We applied this method, and we verified that the 99% of seasons have lengths shorter than seven months. Then, for each cell, we extract fire seasons of seven months centered in the month with the highest occurrence of fire. The global trend shows a decrease in the mean FSS, except in some regions like the west coast of the United States, Northeast Brazil, and East Russia.

We also verified, in this paper, the possibility of predicting worldwide FSS. We applied seven forecasting methods to the FSS from each cell and we observed that the mean absolute error (MAE), for the best method in each cell, is low for many cells. This suggests that it is possible to forecast FSS using just historical FCs. It is important to mention that our study only uses historical data that may not take into account climate change, what may considerably modify the fire seasons in the future. In summary, our results show that the historical data indicates a global decrease in the length and severity of fire seasons, and that is possible to forecast the severity. Our results reinforce the importance of controlling global fire activity and reducing the anthropogenic causes of climate change.

This manuscript is organized in the following form. In Sec. 2, we present the data, our proposed method of fire season estimation, the forecasting methods employed to predict the fire season severity, and the evaluation measures. In Sec. 3, we present our results and discussion divided into three analyses: fire season length, fire season severity, and forecasting. Finally, we present in Sec. 4 some conclusions and future works.

## 2. Material and Methods

### 2.1. Data

In our experiments, we use data from the Moderate Resolution Imaging Spectroradiometer (MODIS) on-board NASA’s Terra and Aqua satellites. Specifically, we used the Global Daily Fire Location Product (MCD14ML) Collection 6 from 2003 to 2017 [5, 6, 7]. It is composed by geographic location, date, detection confidence, and some additional information for each fire pixel detected by the Terra and Aqua MODIS sensors. We consider only those fire records in the data set with detection confidence higher than 75%. We disregard

the years of 2001 and 2002 because they have missing data. The data set is freely accessible [7].

To analyze this spatiotemporal data set, we divide the globe into 65,612 hexagonal grid cells of approximated  $7,774 \text{ km}^2$  each [8]. The main advantage of the hexagonal grid, when compared to the traditional rectangular longitude–latitude one, is that the former generates cells with more uniform coverage area and avoid distortions. Since the vast majority of the grid cells are located in regions without fire, like in the oceans or poles, we discard many cells. Only cells with at least one FC per season were considered. After selecting only those cells with fire, we end up with 6486 ones. For each of those cells, we construct a time series with the daily fire counts detected by the satellites.

## 2.2. Fire Season Estimation

The goal of this paper is to analyze the severity of the fire seasons around the globe. To estimate the length of the fire seasons, we propose a simple method: First, we apply a moving average to smooth the historical time series of fire counts (FC). Then, we count the largest periods without fire. We remove these periods and consider the other ones as fire seasons. In Fig 1, we illustrate this process using three FC time series from different regions.

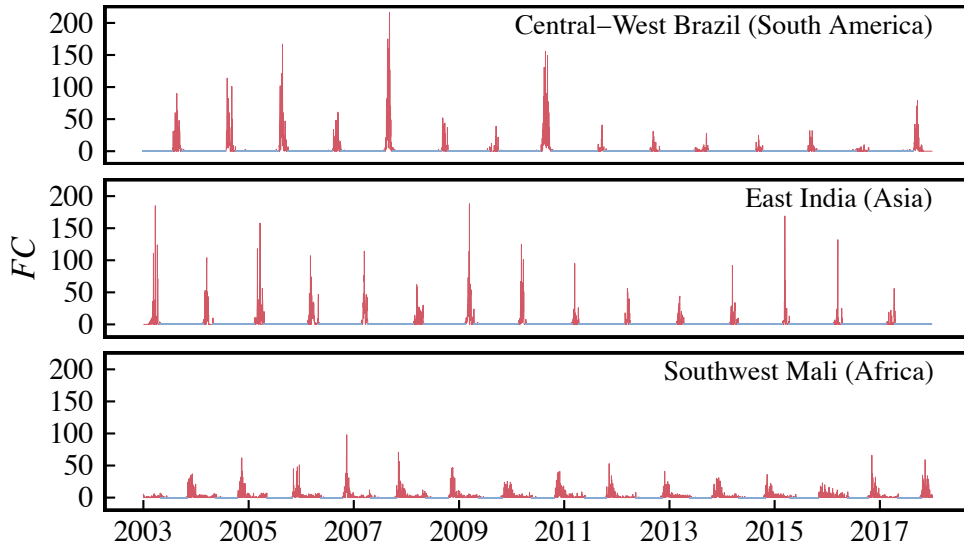


Figure 1: (Color online) Fire seasons estimation. Each time series represents the daily fire counts (FC) detected in grid cells located in three different regions: Brazil, India, and Mali. After the smoothing, we count the periods without fire (in blue) and consider the other periods (in red) as fire seasons.

We define fire seasons as the time window centered in the month with the highest occurrence of fire in each cell [4]. To define a single proper time window length to be used for all the cells, we use the fire season estimation method here proposed. Specifically, this method was applied to the time series from all grid cells and verified the empirical distribution of fire season mean lengths. We choose the 99% season length percentile as the global season length (see Sec. 2.2). This method guaranties that FC time series from all cells have the

same length and well represents the periods with more fire. The fire season severity (FSS) is the sum of fire counts (FC) in season [4].

### 2.3. Forecasting methods and evaluation

To fit the models, we opt for using the monthly-accumulate fire counts (MA-FC) of each season. We discard the first and last season to avoid measuring a broken season. Since every season has 7 months, the MA-FC has 91 values. For each cell, we separate the first 10 seasons from training the model and the other three ones to test. We performed a Box-Cox transformation in both the train and test time series, and the parameter lambda was calculated using the method proposed by Guerrero [9]. In the following, we briefly describe the forecasting methods employed here:

- *Naive forecasting*: one of simplest forecasting methods, it considers the last observation in a non-seasonal time series as the prediction for the next value [10]. In a seasonal time series, the seasonal naive forecasting (snaive) method consider each forecast to be equal to the last observed value from the same season. Although their simplicity, these two methods provide proper results in many cases. We use these methods as baselines.
- *Autoregressive Integrated Moving Average models (ARIMA)*: aims to describe the autocorrelations in the data, and it is one of the most widely used approaches for time series forecasting. The prediction of a variable is assumed to be a linear function of several past observations and random errors. The procedure starts with the AR part, which involves regressing the variable on its own lagged (i.e., past) values. The MA part performs a moving-average of the error term as a linear combination that occurs at different times in the past. In this way, the model provides a suitable description of a stationary stochastic process regarding two polynomials, one for the autoregression (AR) and the second for the moving average (MA). We employ the function in R that uses the Hyndman-Khandakar algorithm for automatic ARIMA modeling, which finds the best AR model and MA weighted linear combination to obtain the model [11].
- *Exponential smoothing (ETS)*: a time series forecasting method that uses a window function to assign exponentially decreasing weights over time. The window function is applied for smoothing the input time series data, acting as low-pass filters to remove high-frequency noise [10]. Thus, the past observations are weighted with a geometrically decreasing ratio, i.e., the more recent the observation, the higher the associated weight. Exponential smoothing methods can be applied to datasets with seasonality and some other prior assumptions, like data with a systematic trend or seasonal component. ETS are well-known forecasting method that may be used as an alternative to the famous ARIMA family of methods. In particular, all ETS models are non-stationary and explicitly uses an exponentially decreasing weight for past observations, while some ARIMA models are stationary and use linear weights sum of past observations as applied in the simple moving average techniques [10].

- *Short-term load forecasting (STLF)*: this approach can be defined as a seasonal and trend decomposition combination using Loess forecasting modeling [11]. These methods assume that a time series can be separated in error, trend and seasonality components. The complete process is divided into decomposition and forecasting, where the first is the input for the second. The time series is decomposed by an MSTL function, which is a variation of a Seasonal and Trend decomposition using Loess (STL) method [12], but designed to deal with multiple seasonality and estimating nonlinear relationships. The returned multiple seasonal components are employed by a naive method for the seasonally adjusted data [11], where the forecasting is nothing but recombining the components. This usually produces quite good forecasts for seasonal time series.
- *TBATS*: it uses a combination of a trigonometric representation of seasonal components based on Fourier terms with an exponential smoothing state space model and Box-Cox transformation [13]. Because it relies on trigonometric functions, it can be used to model non-integer seasonal and higher frequency time series that exhibit more elaborated patterns. As main properties [13], the TBATS modeling framework admits a larger parameter space with the possibility of better forecasts. It allows for the accommodation of nested and non-nested multiple seasonal components and handles typical nonlinear features often seen in real time series. Also, it is robust for any autocorrelation in the residuals, and it involves a much simpler, yet efficient estimation procedure. Besides, the TBATS models can be used as a means of decomposing complex seasonal time series into trend, seasonal and irregular components. In decomposing time series, the trigonometric approach has significant advantages over the traditional forecasting formulations [13].
- *Generalized linear model for count time series (TSGLM)*: count time series take into account that the observations are non-negative integers and the models should capture suitably the dependence among observations. A convenient and flexible technique is to employ the generalized linear model (GLM) approach for modeling the observations conditionally on the past information [14]. In this way, TSGLM is a GLM method that provides likelihood-based estimation for analysis and modeling of count time series [14]. The specification of the linear predictor permits the regression on past values, past observations, and to potential covariate effects. As conditional distributions, it can be selected either Poisson or negative binomial. The linear estimation is carried out by the conditional or quasi-likelihood approach or maximum likelihood for the Poisson distribution for the negative binomial distribution [14].
- *Artificial neural networks (ANN)*: model inspired by the biological neural networks constituted in animal brains. They are based in a set of connected units called artificial neurons [15]. The architecture of ANN frequently contains multilayer perceptron and sigmoid neurons, organized in layers and employing the stochastic gradient descent as the standard of the learning process. The ANNs are trained to learn the input-output relationships through an iterative process, in which the weight of the neurons

are adjusted to minimize the error between the predicted and the true outputs. As a result, it is expected that the ANN learns a suitable model that accurately generalize the response to new data.

- *Prophet*: this is an open source software released by Facebook [16], which is employed in many applications by the company for producing reliable forecasts for planning and goal setting. The algorithm was developed for forecasting time series data based on an additive model where non-linear trends are fit with yearly, weekly, and daily seasonality. The method is based on a decomposable time series model with three main model components [17]: trend, seasonality, and holidays effect. According to the authors, Prophet performs better than any other approach in the majority of cases. Particularly, the proposed time series forecasting model is robust to missing data and shifts in the trend, and typically handles outliers well [17]. It was designed to handle time series that have strong seasonal effects and several seasons of historical data.

In the experiments, we used the R programming language [18] with the packages: **forecast** [11], **prophet** [16], and **tscount** [14]. These packages provide implementations of the forecasting methods and automatically tune the parameters for fitting the models to the time series.

We apply all the mentioned forecasting methods for the MA-FC for each cell. The FSS prediction is the accumulated of the predicted MA-FCs in a season. To find the best forecasting method of a single time series from a grid cell, we compared the mean absolute error (MAE) [10]. Considering an observed (test) time series  $Y$  of  $n$  values and  $F$  the predicted values for  $Y$ , the prediction error  $e_t$  in a time  $t$  is the difference between an observed value and its forecast:  $e_t = Y_t - F_t$ . The MAE is defined as:

$$MAE = n^{-1} \sum_{t=1}^n |e_t|. \quad (1)$$

The scaled forecasting error  $q_t$  of a non-seasonal time series  $Y$  is the error  $e_t$  divided by the MAE of the non-seasonal naive forecast method on the training set:

$$q_t = \frac{e_t}{\frac{1}{n-1} \sum_{t=2}^n |Y_t - Y_{t-1}|}. \quad (2)$$

The scaled error  $q_t$  of a time series  $Y$  with a seasonal period  $m$  is:

$$q_t = \frac{e_t}{\frac{1}{n-m} \sum_{t=m+1}^n |Y_t - Y_{t-m}|}. \quad (3)$$

If  $q_t < 1$ , the forecasting method is better than the seasonal naive (snaive) computed on the training data, otherwise snaive is better.

The mean absolute scaled error (MASE) was used to compare the accuracies of different methods in all cells [19]. As its name indicates, is simply the mean of all scaled errors:

$$MASE = n^{-1} \sum_{t=1}^n |q_t| \quad (4)$$

When  $MASE < 1$ , the forecasting method gives, on average, smaller errors than the one-step errors from the naive method.

In the following, we summarize the forecasting methodology in three steps:

1. *Data*: we use NASA’s global fire count data (MCD14ML Collection 6) from 2003 to 2017. We divide this spatiotemporal data set into hexagonal grid cells and extract daily fire count time series from each cell.
2. *Fire season extraction*: we estimate the fire season length for each cell by counting the largest periods without fire. We remove these periods and consider the other ones as fire seasons. We estimate a length for all the cells and choosing a global time window that better describes all the cells. This length is the 99% percentile of all fire season lengths. After defining the global length, we consider the fire seasons as the time window centered in the months with the highest fire counts of each cell.
3. *Fire season severity forecasting*: seven forecasting methods were applied to find the best method (lowest MAE) for the monthly-accumulate fire counts (MA-FC) in each cell. Different methods were compared using the MASE. The FSS prediction is the accumulated of the months’ predictions in a season.

### 3. Results and Discussion

#### 3.1. Fire season Analysis

We propose in Sec. 2.2, a simple method to estimate the fire season length. In our first analysis, we applied this method to all the grid cells. Since we have 15 years of fire data, we extracted the same amount of fire seasons. We remove in this analyze, the first (2003) and the last (2017) seasons to avoid measuring partial fire seasons. We also removed outlier season lengths, i.e., values higher than the third quartile ( $Q_3$ ) +  $1.5 \times$  interquartile range ( $IQR$ ).

In Fig. 2, we illustrate the mean fire season length and trend for each cell. Some of the regions with the longest (more than 7 months) fire season lengths are Paraguay, Southeast of US, north of Australia, and most parts of Africa. Since 99% of the cells have fire seasons shorter than seven months (in the mean), we consider seven months a reasonable time window to represent worldwide fire seasons. The trends show a global decline in the fire season lengths (57% of cells), except in some regions like the Northeast Brazil, Eastern Russia, and parts of Africa.

After defining seven months as the fire season length, we find the months with highest occurrence of fire in each cell. Fig. 3 shows the months with peaks of fire activity and a histogram with the months’ distribution (inset). The months of maximum fire activity are distributed following a bimodal distribution, which mainly represents the dry seasons in the tropical rain belt (northern to the southern tropics). In the tropical zone, regions below the

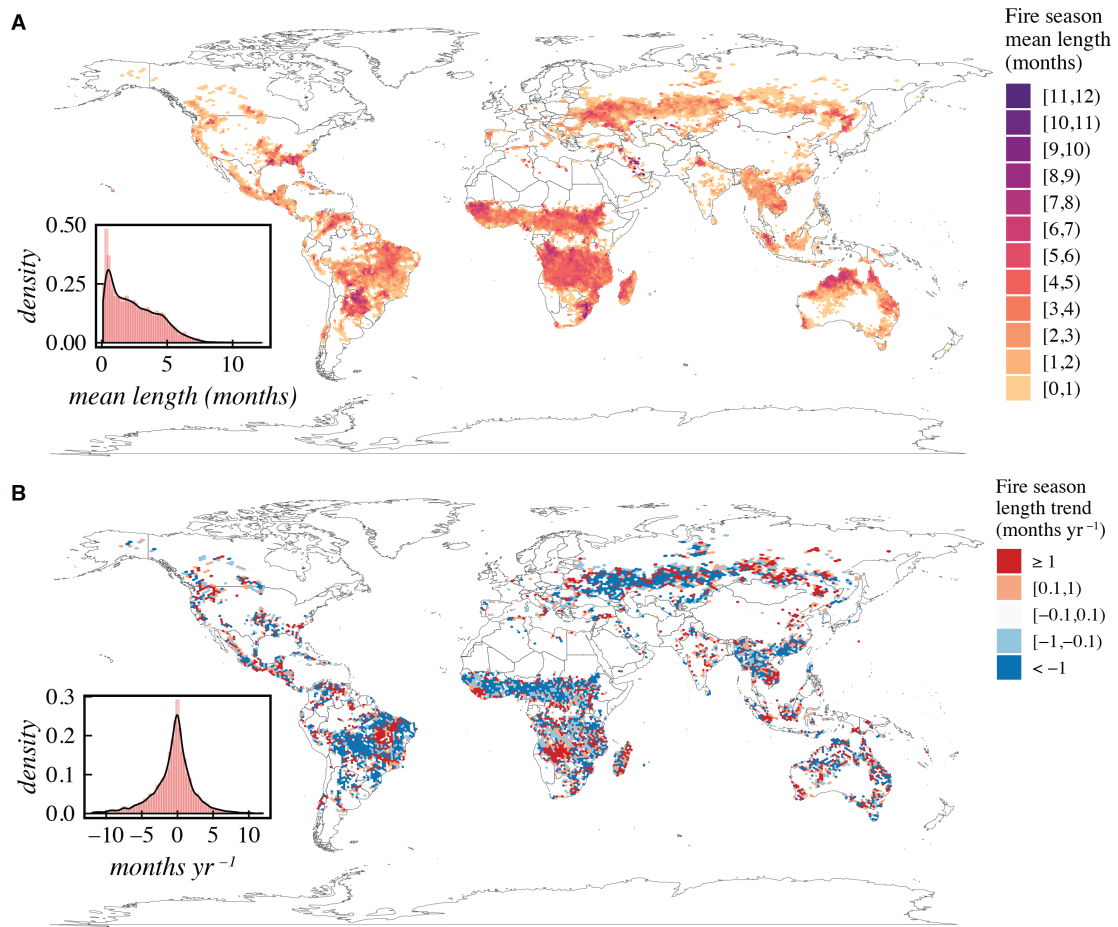


Figure 2: (Color online) Global Fire season length means (A) and trends (B). The inset figures show the respective probabilistic density functions (PDF).

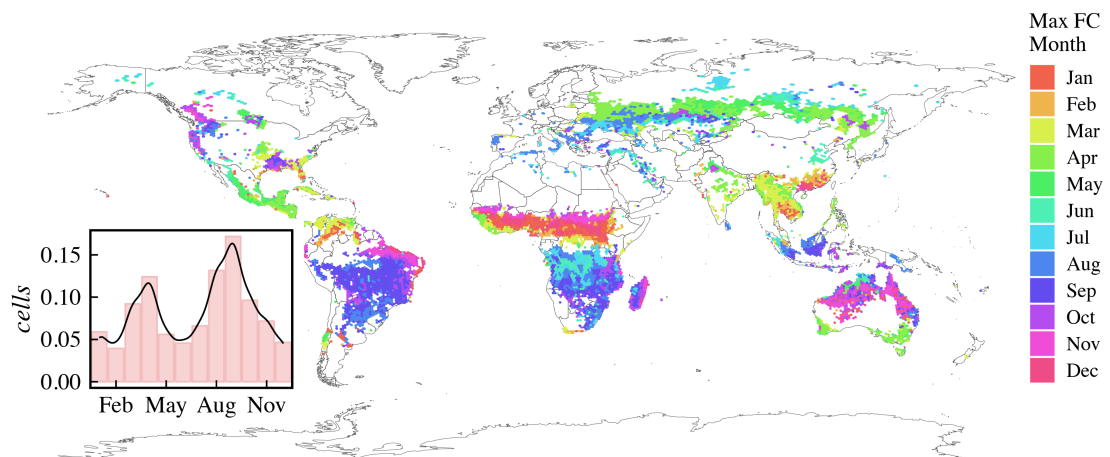


Figure 3: (Color online) Months with the highest fire activity in each cell. The inset figure shows a histogram with the number of cells with the highest fire activity in a month.



Equator have peaks of fire activity between August and October while locations above the Equator have maximums between March and May. Right on the equator, the fire activity is predominant in the end of the year (November to January). Part of the high fire activity in April is accounted for the dry seasons in parts of Russia and South Australia [20].

The fire seasons are the periods of seven months centered in the month with the highest occurrence of fire in In Fig. 4, we show the fire season severity (FSS) means and trends calculated for all the cells. In both measures, we removed the first (2003) and the last (2017) seasons to avoid measuring partial fire seasons. 50% of the global area have FSS mean lower than 100 FCs per year and 99% have less than 1200 mean FCs. The tropics concentrate the highest number of fire counts. In general, there is a trend of decline in the mean FSS worldwide (61% of cells), except in regions like the Southern Africa, Far Eastern Russia, Eastern Ukraine, and the West Coast of USA.

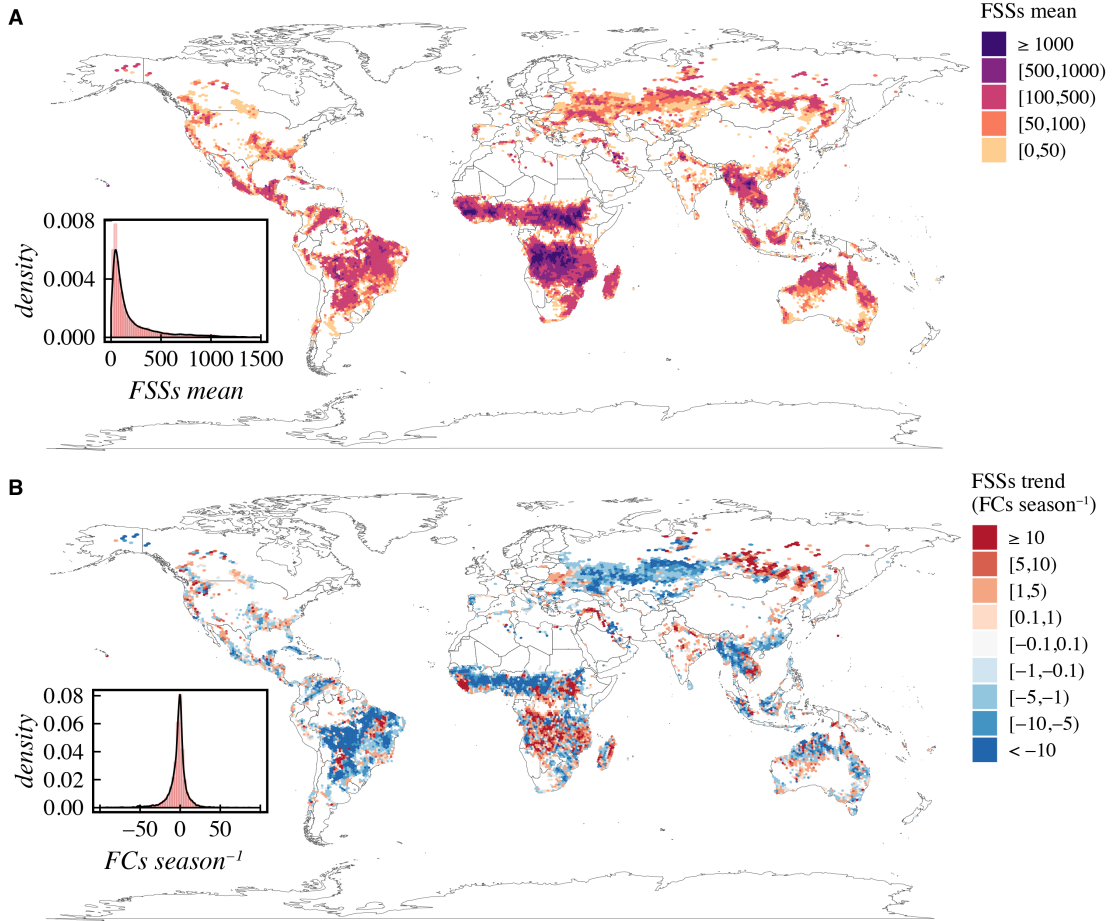


Figure 4: (Color online) Global Fire season severity (FSS) means (A) and trends (B). The inset figures show the respective probabilistic density functions (PDF).

There are several reasons that explain the trends in the fire seasons lengths and severity. The main elements related to those variations are the increase or decrease of factors that lead to fire ignitions, such as less deforestation or lower lightning occurrence. They may also be

decreasing flammability conditions with more rainfall. Climate change has also an important influence in the fire regimes [21]. The increase in population densities and cropland areas can also lead to a decrease in the global burnt area [22]. Other factors are the possible decrease in the biomass that can be burned or an increase in fire control and management.

### 3.2. Fire season severity forecasting

The goal of this paper is to apply time series forecasting methods to estimate the fire season severity (FSS). As described in Sec. 2, we use the monthly-accumulated fire count (MA-FC) time series to train seven forecasting methods (Sec. 2.3) for each cell. The intention is to verify if it is possible to forecast MA-FC with low error.

The forecasting results are illustrated in Fig. 5. On the top figure (5-A), we show the MAE for best method and the density function for the MAE (inset). We used the 10 first seasons to train the models and the last three ones to calculate the MAEs. Outliers were removed ( $> Q_3 + 1.5 \times IQR$ ). For 50% of the time series, the MAE is lower than 8 fire counts, what indicates a low general error. However, in some regions with high mean FSS (Fig. 4), like the Northern Australia and parts of Africa, the error is high.

In the bottom figure (5-B), we present a boxplot of the MASE for the entire world divided by continent. Outliers were removed ( $> Q_3 + 1.5 \times IQR$ ). The TBATS and the

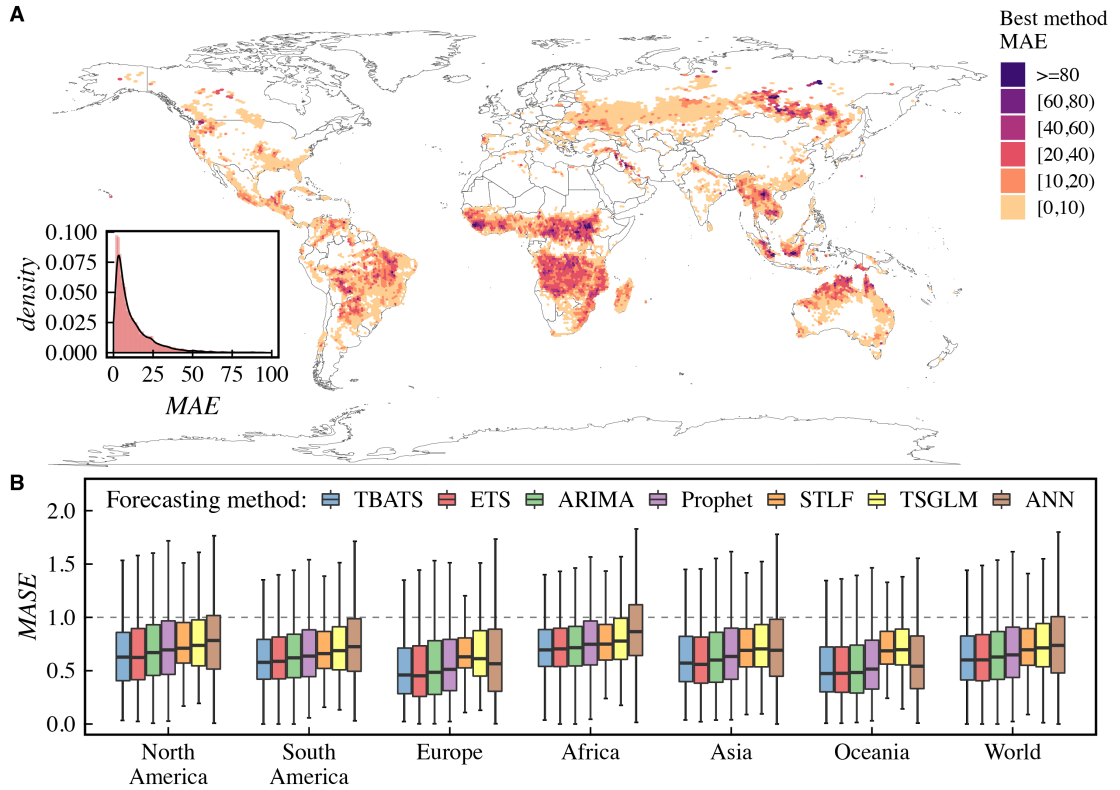


Figure 5: (Color online) Monthly-accumulated fire counts (MA-FC) forecasting. (A) The MAE from the best model for each cell and the PDF (inset). (B) Models comparison using the MASE (Eq. 3) for the seasonal MA-FC from each cell divided by continent and the global (outliers removed).

ANN models present the lowest and the highest median error respectively. TBATS provides statistically better (Friedman and Nemenyi tests  $p$ -value  $< 0.001$  [23]) than the others, except ETS. In 75% of the time series, the forecasting methods provide results better ( $MASE < 1$ ) than a seasonal naive forecasting method in almost all the regions.

Our results show that MAEs and MASEs for the MA-FC time series are low, what suggests that it is possible to apply this data to forecast fire seasons severities. In our next analyses, we use the best model for each cell to predict FSS. The FSS is the accumulate of the predicted fire counts in a season.

In Fig. 6, we present the MAEs and MASEs achieved comparing the best model for each cell with the forecasting results from a linear regression. When comparing the MAEs with the mean FSSs (Fig. 4) we can observe regions where the MAEs are relatively low. For example, in Africa, where the FSS means exceed 400 fire counts, the median MAEs are 45 FCs (outliers removed). For half of the cells, the MAEs are lower than 34 FCs. This result suggests the predictability of FSSs in some regions.

Different from the previous analysis, here the MASEs were calculated considering a non-seasonal time series (Eq. 2). Outliers were removed ( $> Q_3 + 1.5 \times IQR$ ). Except

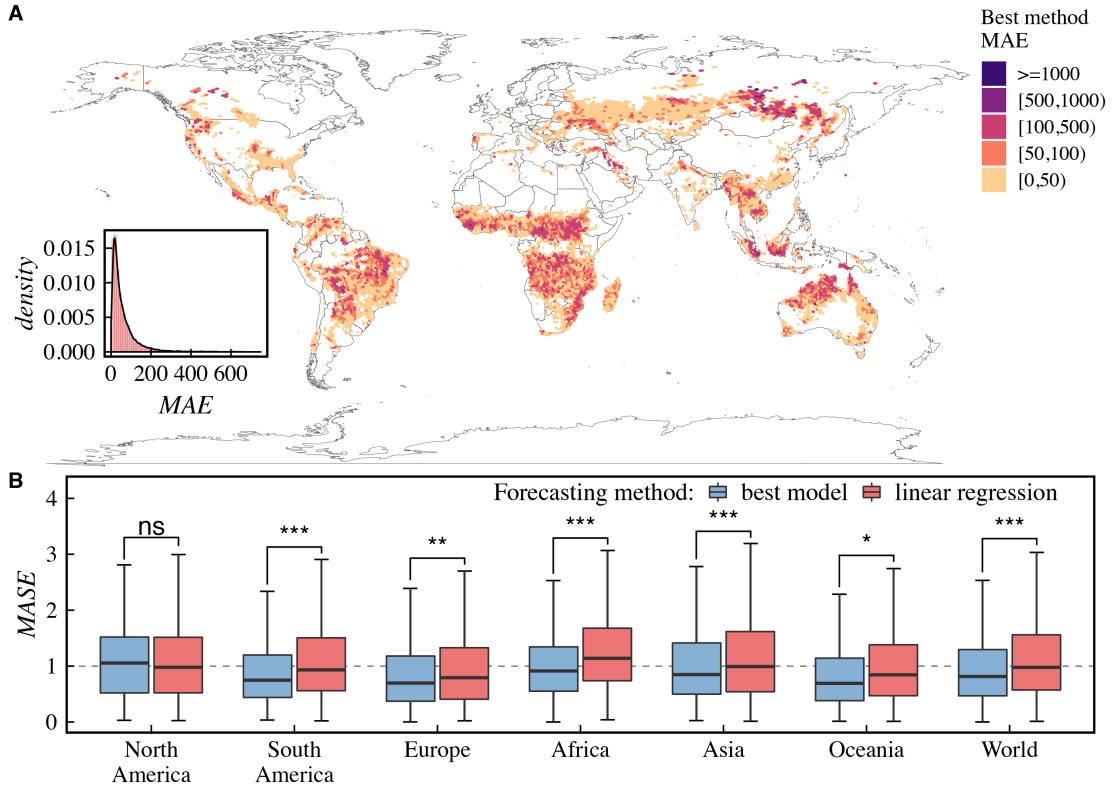


Figure 6: (Color online) FSS forecasting. (A) The MAE from the best model for each cell and the PDF (inset). (B) Forecasting comparison between the best model achieved with MA-FCs and the linear regression in each cell. Accuracy was measured using the MASE (Eq. 3) for the non-seasonal FSS from each cell divided by continent and the global (outliers removed).

for the North America, the median MASEs are lower than one for the best models, what indicates that predictions are better than naive forecasting method in at least 50% of the cells. The best models for each cell statistically (Wilcoxon paired test [23]) outperform the linear regression, except in North America where the errors are not statistically different. This result reinforces the predictability of FSSs in some regions.

#### 4. Conclusions

In this paper, we have analyzed global fire season severity, defined here as the accumulated of fire counts detections in a season. We divided the globe into hexagonal grid cells and extracted time series of fire counts in each cell. We proposed a very simple method to estimate the fire seasons. Our results show that 99% of the cells have seasons shorter than seven months. We observed that the length of fire seasons are decreasing in general, except in Southern Africa, Northeast Brazil and East Russia. The global FSS is also declining in general, excluding some regions like the Southern Africa, Far Eastern Russia, Eastern Ukraine, and the West Coast of USA. One explanation for the declining fire activity is the Agricultural expansion and intensification [3].

We also show that it is possible to forecast FSS in some regions. Since FSS time series are very short, we used the monthly-accumulated fire counts (MA-FC) to train and test seven forecasting models. The mean absolute error (MAE) for the MA-FC is lower than 8 fire counts in more than 50% of the cells. It is a low error compared to the high FSSs means observed in the historical data. In general, the TBATS forecasting model provides the best results. The mean absolute scaled error (MASE) is lower than one in more than 75% of the cells. It indicates that the best models for each cell provide more accurate results than the naive forecasting method. According to the MAEs and MASEs, we conclude that it is possible to predict FSS in some regions using MA-FC.

Finally, we compared the FSS predictions for the best methods (using MA-FC) for each cell with a linear regression method. Again, we observe that MAEs and MASEs are relatively low. The MASEs are lower than the one in as least 50% of the cells. The MASEs achieved with the best models are statistically lower than the linear regression, except in North America, where no statistical difference was observed. Therefore we conclude that many regions present predictable variations in the FSS.

It is important to mention that our results are based on the historical data, which is short and limited. Our results are aligned with previous results [3, 22]. However, they might not reflect the future if the climate keeps changing. Some previous results suggest an increase in fire activity in some regions [24, 25]. Since our results point to a global decrease in fire activity, we consider that they reinforce the importance of controlling fire activity and reducing the anthropogenic causes of climate change.

This work can be extended in many directions. In this paper, we focused in a global analysis, but a natural next step is the thorough analyses of specific regions and the deep reasons that explains fire activity variations. Other forecasting methods and machine learning tasks can also be explored on this data set. Tasks including fire seasons classification,

clustering, and anomaly detection. These techniques might reveal new patterns about the interplay between anthropogenic activity and global fire dynamics.

## Acknowledgments

This research is supported by the Fundação de Amparo à Pesquisa do Estado de São Paulo (FAPESP) under Grant No.: 2015/50122-0 and the German Research Council (DFG-GRTK) Grant No.: 1740/2. L. N. F. thanks FAPESP Grant No.: 2017/05831-9 and D.A.V.O acknowledges FAPESP Grants 2016/23698-1, 2018/01722-3, and 2018/24260-5. This research was developed using computational resources from the Center for Mathematical Sciences Applied to Industry (CeMEAI) funded by FAPESP (grant 2013/07375-0).

## References

- [1] D. M. Bowman, J. K. Balch, P. Artaxo, W. J. Bond, J. M. Carlson, M. A. Cochrane, C. M. D’Antonio, R. S. DeFries, J. C. Doyle, S. P. Harrison, F. H. Johnston, J. E. Keeley, M. A. Krawchuk, C. A. Kull, J. B. Marston, M. A. Moritz, I. C. Prentice, C. I. Roos, A. C. Scott, T. W. Swetnam, G. R. Van Der Werf, S. J. Pyne, Fire in the earth system, *Science* 324 (2009) 481–484.
- [2] S. S. Rabin, J. R. Melton, G. Lasslop, D. Bachelet, M. Forrest, S. Hantson, J. O. Kaplan, F. Li, S. Mangeon, D. S. Ward, C. Yue, V. K. Arora, T. Hickler, S. Kloster, W. Knorr, L. Nieradzik, A. Spessa, G. A. Folberth, T. Sheehan, A. Voulgarakis, D. I. Kelley, I. C. Prentice, S. Sitch, S. Harrison, A. Arneth, The fire modeling intercomparison project (firemip), phase 1: experimental and analytical protocols with detailed model descriptions, *Geoscientific Model Development* 10 (2017) 1175–1197.
- [3] N. Andela, D. C. Morton, L. Giglio, Y. Chen, G. R. van der Werf, P. S. Kasibhatla, R. S. DeFries, G. J. Collatz, S. Hantson, S. Kloster, D. Bachelet, M. Forrest, G. Lasslop, F. Li, S. Mangeon, J. R. Melton, C. Yue, J. T. Randerson, A human-driven decline in global burned area, *Science* 356 (2017) 1356–1362.
- [4] Y. Chen, J. T. Randerson, D. C. Morton, R. S. DeFries, G. J. Collatz, P. S. Kasibhatla, L. Giglio, Y. Jin, M. E. Marlier, Forecasting fire season severity in south america using sea surface temperature anomalies, *Science* 334 (2011) 787–791.
- [5] C. Justice, J. Townshend, E. Vermote, E. Masuoka, R. Wolfe, N. Saleous, D. Roy, J. Morisette, An overview of modis land data processing and product status, *Remote Sensing of Environment* 83 (2002) 3 – 15.
- [6] L. Giglio, W. Schroeder, C. O. Justice, The collection 6 modis active fire detection algorithm and fire products, *Remote Sensing of Environment* 178 (2016) 31 – 41.
- [7] L. Giglio, MODIS Collection 6 Active Fire Product User’s Guide Revision A, [http://modis-fire.umd.edu/files/MODIS\\_C6\\_Fire\\_User\\_Guide\\_A.pdf](http://modis-fire.umd.edu/files/MODIS_C6_Fire_User_Guide_A.pdf), 2019. [Online; accessed 01-March-2019].
- [8] R. Barnes, dggridR: Discrete Global Grids for R, 2017. R package version 2.0.1.
- [9] V. M. Guerrero, Time-series analysis supported by power transformations, *Journal of Forecasting* 12 (1993) 37–48.
- [10] R. Hyndman, G. Athanasopoulos, *Forecasting: principles and practice*, OTexts, 2018.
- [11] R. J. Hyndman, Y. Khandakar, Automatic time series forecasting: the forecast package for R, *Journal of Statistical Software* 26 (2008) 1–22.
- [12] R. B. Cleveland, W. S. Cleveland, J. E. McRae, I. Terpenning, Stl: A seasonal-trend decomposition procedure based on loess, *Journal of Official Statistics* 6 (1990) 3–73.
- [13] A. M. D. Livera, R. J. Hyndman, R. D. Snyder, Forecasting time series with complex seasonal patterns using exponential smoothing, *Journal of the American Statistical Association* 106 (2011) 1513–1527.
- [14] T. Liboschik, K. Fokianos, R. Fried, tscount: An r package for analysis of count time series following generalized linear models, *Journal of Statistical Software, Articles* 82 (2017) 1–51.

- [15] C. M. Bishop, *Neural Networks for Pattern Recognition*, Oxford University Press, Inc., New York, NY, USA, 1995.
- [16] S. Taylor, B. Letham, prophet: Automatic Forecasting Procedure, 2018. R package version 0.3.0.1.
- [17] S. J. Taylor, B. Letham, Forecasting at scale, *PeerJ Preprints* 5 (2017) e3190v2.
- [18] R Core Team, *R: A Language and Environment for Statistical Computing*, R Foundation for Statistical Computing, Vienna, Austria, 2017.
- [19] R. J. Hyndman, A. B. Koehler, Another look at measures of forecast accuracy, *International Journal of Forecasting* 22 (2006) 679 – 688.
- [20] M. C. Peel, B. L. Finlayson, T. A. McMahon, Updated world map of the köppen-geiger climate classification, *Hydrology and earth system sciences discussions* 4 (2007) 439–473.
- [21] R. Kelly, M. L. Chipman, P. E. Higuera, I. Stefanova, L. B. Brubaker, F. S. Hu, Recent burning of boreal forests exceeds fire regime limits of the past 10,000 years, *Proceedings of the National Academy of Sciences* 110 (2013) 13055–13060.
- [22] V. K. Arora, J. R. Melton, Reduction in global area burned and wildfire emissions since 1930s enhances carbon uptake by land, *Nature Communications* 9 (2018) 1326.
- [23] J. Demšar, Statistical comparisons of classifiers over multiple data sets, *J. Mach. Learn. Res.* 7 (2006) 1–30.
- [24] M. Flannigan, A. S. Cantin, W. J. de Groot, M. Wotton, A. Newbery, L. M. Gowman, Global wildland fire season severity in the 21st century, *Forest Ecology and Management* 294 (2013) 54 – 61.
- [25] L. E. O. C. Aragão, L. O. Anderson, M. G. Fonseca, T. M. Rosan, L. B. Vedovato, F. H. Wagner, C. V. J. Silva, C. H. L. Silva Junior, E. Arai, A. P. Aguiar, J. Barlow, E. Berenguer, M. N. Deeter, L. G. Domingues, L. Gatti, M. Gloor, Y. Malhi, J. A. Marengo, J. B. Miller, O. L. Phillips, S. Saatchi, 21st century drought-related fires counteract the decline of amazon deforestation carbon emissions, *Nature Communications* 9 (2018) 536.